BARRIER CROSSING INDUCED BY FRACTIONAL GAUSSIAN NOISE

O.YU. SLIUSARENKO,[1] V.YU. GONCHAR,[1] A.V. CHECHKIN[1,2]

[1]National Science Center "Kharkiv Institute of Physics and Technology", Akhiezer Institute for Theoretical Physics
(1, Akademichna Str., Kharkiv 61108, Ukraine)

[2]School of Chemistry, Tel Aviv University
(Ramat Aviv 69978, Tel Aviv, Israel)

PACS 05.40.Fb, 02.50.Ey, 82.20.-w

A problem of the rate of escape of a particle under the influence of the external fractional Gaussian noise is studied by using the method of numerical integration of an overdamped Langevin equation. Considering a truncated harmonic potential, the dependences of the mean escape time on the noise intensity and Hurst index are evaluated, together with the probability density functions for the escape times. It is found that, like the corresponding classical problem with white Gaussian noise, they both obey an exponential law.

1. Introduction

The problem of a Brownian particle's escape rate arises in a lot of natural processes in physics, chemistry, and biology, such as diffusion in solids, homogeneous nucleation, electrical transport theory, chemical kinetics, unfolding of proteins *etc.* (see, e.g., [1, 2] and references therein). The first attempt to describe the process was made by S. Arrhenius [3], who introduced the rate coefficient k and noticed the dependence

$$k = \nu \exp(-\beta E_b), \tag{1}$$

where ν and β are constants, and E_b is the activation energy. Since is was realized that the escapes could happen due to thermal noise, the further development of the problem awaited the creation of a consistent fluctuation theory, attaining the second birth after the works of Smoluchowski [4]. First, the problem was studied in [5], the seminal papers on the rate theory were written by H. Kramers [6] (now the problem of the escape rate is also known as the Kramers problem) and S. Chandrasekhar [7], nowadays being included in almost every textbook on statistical physics in that "classical" form. Later on, it was re-considered using different approaches and in more details (see e.g. [2, 8]).

However, the theory of Brownian motion cannot explain anomalous diffusion phenomena which are widely observed in various physical (Sinai diffusion [9], turbulent Richardson flow [10, 11], motion of charge carriers in amorphous semiconductors [12, 13]), biological (motion in biological cells [14, 15]), biochemical (the spreading of tracer molecules in subsurface hydrology [16]), chemical, and geophysical systems [17]. In such systems, the mean squared displacement of a particle does not obey a regular diffusion law

$$\left\langle x^2(t)\right\rangle = 2D_H t^{2H}, \tag{2}$$

where D_H is a generalized diffusion coefficient, H is Hurst exponent varying between 0 and 1. The case where $H > 1/2$ (the mean squared displacement grows faster than t^1) is called superdiffusion; when $H < 1/2$, we have a subdiffusion phenomenon.

Despite the "symptoms" of systems may be the same, the anomalous diffusion has several mechanisms. The most discussed ones nowadays are the continuous time random walks and the fractional Brownian motion models. The former implies either subdiffusion (while walking, the particle experiences long periods of rest, so that the waiting times have an infinite characteristic time) or superdiffusion (e.g., Lévy flights, when the mean squared displacement diverges, but the waiting times are finite). The Kramers problem for Lévy flights was considered in [17–20].

The second model (fractional Brownian motion) was suggested by Kolmogorov in 1940 [21] and later reconsidered by Mandelbrot and van Ness [22]. They defined the fractional Brownian motion as a self-similar stochastic process, whose formal derivative $\xi_H(t)$ called the fractional Gaussian noise is a stationary random process with long memory effects. Namely, its autocorrelation function in the discrete time approximation has the form

$$\langle \xi_H(0)\xi_H(j)\rangle = D_H\left(|j+1|^{2H} - 2|j|^{2H} + |j-1|^{2H},\right). \tag{3}$$

where j is an integer. At large j corresponding to a long-time asymptotics, the autocorrelation function de-

cays as $\langle \xi_H(0)\xi_H(t)\rangle \simeq 2D_H H(2H-1)t^{2H-2}$, $H \neq 1/2$, thus showing a long power-law memory. The "ordinary" Brownian limit corresponds to $H = 1/2$, and $\langle \xi_{1/2}(t_1)\xi_{1/2}(t_2)\rangle = 2D\delta(t_1 - t_2)$.

Despite its wide use, the fractional Brownian motion is not completely understood, since still there are no consistent analytical methods. However, the development of modern computational devices allows one to investigate the stochastic systems with such diffusion mechanisms, by using various numerical simulation techniques. Thus, the fractional Brownian motion is used to model a variety of processes including the monomer diffusion in a polymer chain [23], single file diffusion [24], diffusion of biopolymers in the crowded environment inside biological cells [25], long-term storage capacity in reservoirs [26], climate fluctuations [27], econophysics [28], and teletraffic [29].

Due to such substantial quantity of applications, the further development of both analytical and simulation approaches is promising.

In this paper, we consider a generalization of the barrier crossing problem by using a numerical method of integrating the overdamped Langevin equation with a fractional Gaussian random source $\xi_H(t)$:

$$\frac{dx}{dt} = -\frac{dU}{dx} + D^{1/2}\xi_H(t), \tag{4}$$

where $x(t)$ is particle's coordinate, $U(x)$ is the potential, $\xi_H(t)$ is the fractional Gaussian noise with intensity D, and H stands for the Hurst index.

We also stress that, in our Langevin description, the fluctuation–dissipation theorem does not hold, as it will be seen below. Therefore, our model is different from that analyzed in [30] and [31]. On the other hand, our approach is similar to that of paper [32]; however, the autocorrelation function of the long-correlated Gaussian noise used there is different from that for the fractional Gaussian noise.

2. Simulation Details

For a simulation, we will need a reliable fast generator of random fractional Gaussian numbers $\xi_H(t)$ (see Eq. (4)). Since the generators provide usually good results either for $H < 1/2$ (antipersistent case) or for $H > 1/2$ (persistent case), we choose two separate ones for each of cases.

The fastest, precise enough (see the tests below), and free of edge effects fractional Gaussian noise generator for the *antipersistent* case is described in [33]. In brief, the idea is as follows.

First, we define a function

$$R_x(n) = \begin{cases} 2^{-1}\left[1 - (n/N)^{2H}\right], & \text{for } 0 \le n \le N, \\ R_x(2N-n), & \text{for } N < n < 2N, \end{cases} \tag{5}$$

where H is the Hurst parameter, $0 < H < 1/2$; n is the step number, and N is the random sample length.

Second, we perform the Fourier transformation of Eq. (5): $S_x(k) = F\{R_x(n)\}$.

Next, we define

$$X(k) = \begin{cases} 0, & \text{for } k = 0, \\ \exp(i\theta_k)\xi(k)\sqrt{S_x(k)}, & \text{for } 0 < k < N, \\ \xi(k)\sqrt{S_x(k)}, & \text{for } k = N, \\ X^*(2N-k), & \text{for } N < k < 2N, \end{cases} \tag{6}$$

where * stands for the complex conjugation, θ_k are uniform random numbers from $[0, 2\pi)$, $\xi(k)$ are Gaussian random variables with the zero mean and the variance equal to 2, and all random variables are independent of one another.

Finally, $y(n) = x(n) - x(0)$, where $x(n) = F^{-1}X(k)$ is the inverse Fourier transformation of Eq. (6), represents a free fractional Brownian trajectory which is to be differentiated with respect to the time in order to get fractional Gaussian random numbers. Since the variance $\langle \xi^2 \rangle$ depends on N, it should be normalized so that $\langle \xi^2 \rangle = 2$.

For the persistent case, we use a generator exploiting the spectral properties of a fractional Gaussian noise [34].

– First, take a white Gaussian noise $\xi(t)$, t is an integer.
– Take the Fourier transformation of it: $S(k) = F\{\xi(t)\}$.
– Multiply it by $1/\omega^{H-1/2}$, $1/2 < H < 1$.
– Make the inverse Fourier transformation, so that $\xi_H(t) = F^{-1}\{S(k)/\omega^{H-1/2}\}$ is supposed to approximate a fractional Gaussian noise with index H.
– Normalize it.

A set of tests of the generators was performed to verify the correctness of the program and to determine the validity limits of the algorithm itself at various values of parameters.

The first and the most natural is the verification of the autocovariance function of the noise (Eq. (3)) with $D = 1$ and $C(j) \equiv \langle \xi_H(0)\xi_H(j)\rangle$:

The second test is the calculation of the mean squared displacement of a free fractional Brownian particle, whose results are omitted in the present paper as trivial.

More spectacular is the test of the mean squared displacement of a particle in an infinite harmonic potential well. We start from the overdamped Langevin equation

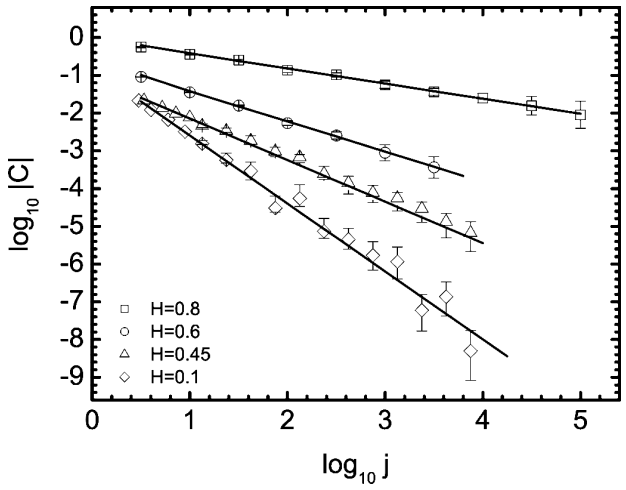

Fig. 1. Autocovariance function of a fractional Gaussian noise, persistent and antipersistent cases, a log-log scale. Squares, circles, triangles, and rhombi with error bars are the simulation data for H=0.8, 0.6, 0.45, and 0.1, respectively. Solid lines provide the linear fitting with Eq. (3)

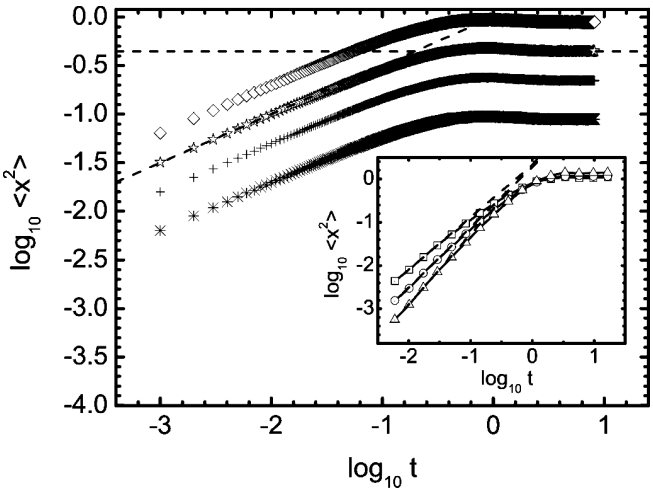

Fig. 2. Mean squared displacement of a particle inside a harmonic potential well. Main graph: antipersistent case, $H = 0.25$ and D=0.1, 0.25, 0.5, and 1.0 (upward). Inset: persistent case, D=1.0 and H=0.8, 0.7, and 0.6 (upward). Points are the simulation data; dashed lines are the asymptotes $\lim_{t\to 0}\langle x^2(t)\rangle \propto t^{2H}$ and $\lim_{t\to\infty}\langle x^2(t)\rangle = D\Gamma(1+2H)$

(4) with the potential $U(x) = ax^2/2$. In dimensionless variables, we get

$$x_{n+1} - x_n = -x_n\delta t + D^{1/2}\delta t^H \xi_H(n). \tag{7}$$

The results of simulations and their comparison with analytical asymptotes are shown in Fig. 2.

Finally, we verify whether the particle's mean escape time from a semiaxis matches the analytical scaling suggested in [35]:

$$p(t) \propto t^{-2+H}. \tag{8}$$

Setting $U(x) \equiv 0$ in Eq. (4), we come to the following discrete-time dimensionless Langevin equation:

$$x_{n+1} - x_n = \delta t^H \xi_H(n). \tag{9}$$

Now, the simulation procedure for the mean escape time is as follows (see the sketch in the inset in Fig. 3):
– Place a "particle" into the starting point ($x = 0$).
– Begin the iterations of Eq. (9).
– Stop the iterations when the "particle" reaches the absorbing boundary at $x_0 = 1$.
– Remember the time of this escape event.
– Re-execute these steps for 100,000 times and average the escape times.

The results demonstrate a good coincidence with Eq. (8) (see Fig. 3). Here, the time step δt= 0.01.

Thus, after ascertaining the work of the algorithm and the generators properly, we pass directly to the main problem. Due to the presence of two different random fractional Gaussian noise generators and different typical time scales for the persistent and antipersistent cases, it is natural to subdivide the further description into two parts.

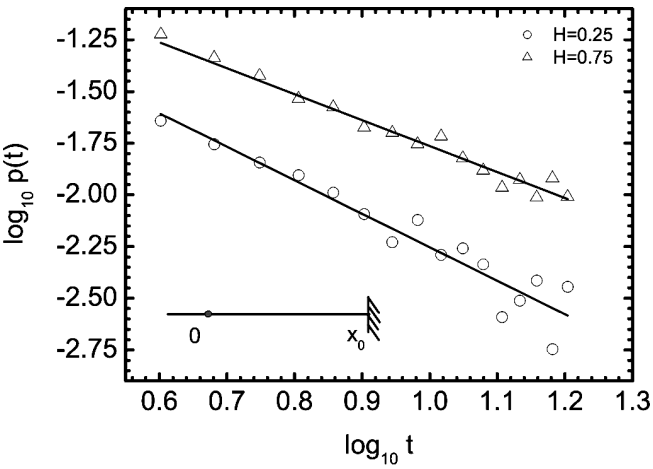

Fig. 3. Verification of the analytical scaling of the free semiaxis mean escape time for a fractional Brownian motion suggested in [35] (solid lines). Circles and triangles represent the simulation results for $H = 0.25$ and $H = 0.75$, respectively. The inset explains the simulation algorithm

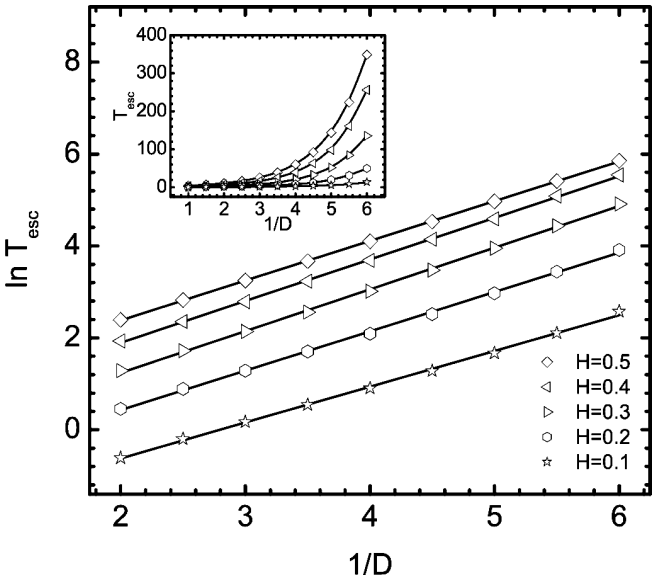

Fig. 4. Mean escape time for a fractional Gaussian noise in the antipersistent case as a function of the noise intensity, a log plot (main panel) and a linear plot (inset). The points show the simulation data (the inaccuracies are of points' size magnitude), the solid lines demonstrate the fitting with Eq. (10)

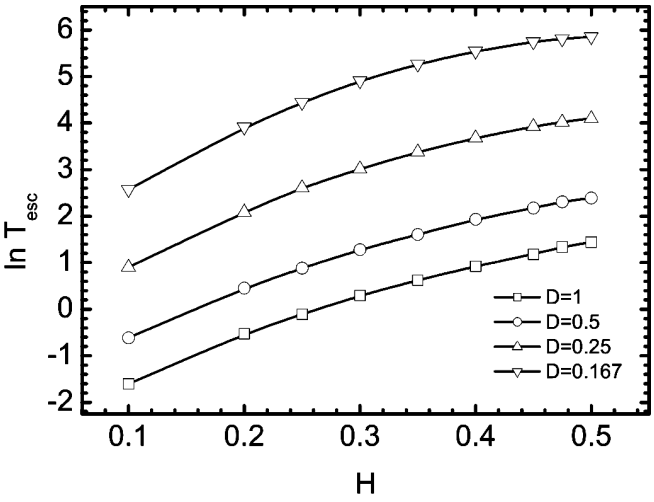

Fig. 5. Mean escape time for a fractional Gaussian noise in the antipersistent case as a function of the Hurst index, a log plot. The points show the simulation data (the inaccuracies are of points' size magnitude), the solid lines demonstrate the fitting with Eq. (10)

3. Antipersistent Case

When dealing with a simulation of the escape problem, two moments are of major importance: the proper selection of a time step (δt) and a set capacity (N). The latter is the generator's parameter that determines the number of random variables in a sample, within which they are correlated with one another. The only way to evaluate them correctly is to simulate some sample paths with arbitrary δt (small enough compared to time scales) and N (large enough). Varying them, we should achieve a satisfactory relationship between the time needed for the simulations and the accuracy. Certainly, they may be different for each pair of the noise intensity and the Hurst parameter.

In the following simulations, we take the time step δt=0.001, and the set capacity varies from $N = 2^{13}$ to $N = 2^{20}$. Again, starting from Eq. (7), we perform the common procedure of evaluating the mean escape time:
– Place a "particle" into the starting point ($x = 0$).
– Begin the iterations of Eq. (7).
– Stop the iterations, when the "particle" reaches the edge of the potential $x_0 = \sqrt{2}$.
– Remember the time of this escape event.
– Re-execute these steps for 100,000 times and average the escape times.

The results are shown in Figs. 4 and 5 below.

As clearly seen from Fig. 4, the data points of the mean escape time dependence on the noise intensity may be nicely fitted with an exponential function, so we introduce the coefficients $a_A(H)$ and $b_A(H)$ (the indices A here indicate the antipersistent case):

$$T_{\rm esc} = \exp(a_A + b_A/D),$$

or

$$\ln T_{\rm esc} = a_A(H) + b_A(H)\frac{1}{D}. \tag{10}$$

The quantity $a_A(H)$ may be fitted well with a linear dependence

$$a_A(H) = a'_A + a''_A H, \tag{11}$$

while $b_A(H)$ is better fitted with a function

$$b_A(H) = b'_A + b''_A H + b'''_A H^2, \tag{12}$$

where $a'_A = -3.019$, $a''_A = 7.296$, $b'_A = 0.705$, $b''_A = 1.489$ and $b'''_A = -2.281$.

The escape times probability density function is simulated almost in the same way as the mean escape time. But, instead of averaging the escape times at the last step, we handle them with a routine that constructs the probability density function. Again, like the classical Kramers problem with a white Gaussian noise source, the escape times probability density function obeys an exponential law (see Fig. 6):

$$p(t) = \frac{1}{T_{\rm esc}} \exp(-t/T_{\rm esc}). \tag{13}$$

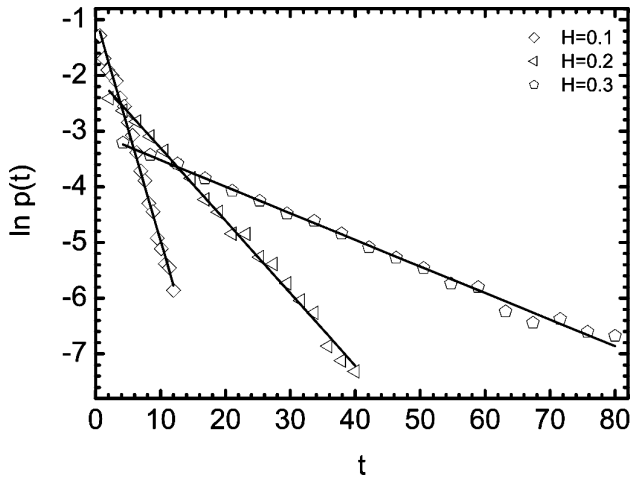

Fig. 6. Escape times probability density function as a function of the walking time, the antipersistent case. The points show the simulation data, the solid lines demonstrate the fitting with Eq. (13)

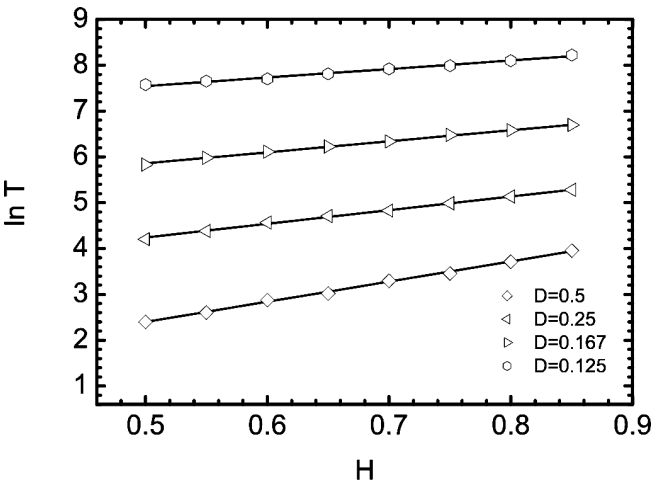

Fig. 8. Mean escape time for a fractional Gaussian noise in the persistent case as a function of the Hurst index, a log plot. The points show the simulation data (the inaccuracies are of points' size magnitude), the solid lines demonstrate the fitting with Eq. (14)

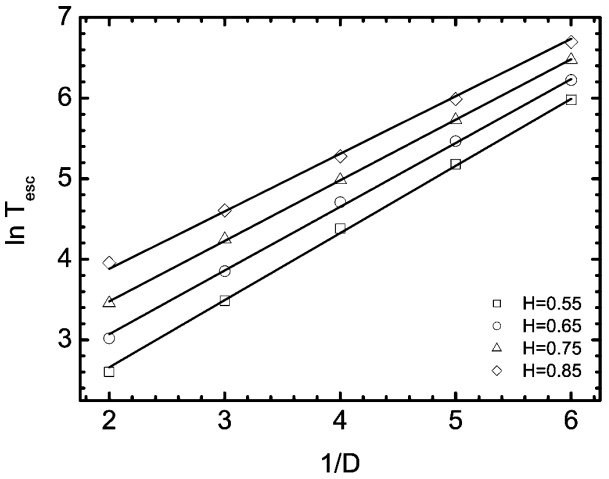

Fig. 7. Mean escape time for a fractional Gaussian noise in the persistent case as a function of the noise intensity, a log plot. The points show the simulation data (the inaccuracies are of points' size magnitude), the solid lines demonstrate the fitting with Eq. (14)

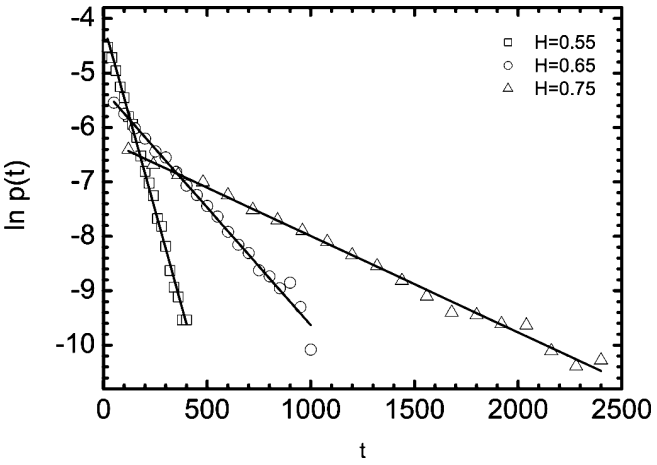

Fig. 9. Escape times probability density function as a function of the walking time, the persistent case. The points show the simulation data, the solid lines demonstrate the fitting with Eq. (13)

4. Persistent Case

Here, the procedures are completely the same, with only slight differences in fittings.

Figure 7 shows the mean escape time dependence on the noise intensity, which is again exponential:

$$\ln T_{\rm esc} = a_P(H) + b_P(H)\frac{1}{D}. \qquad (14)$$

Now, both $a_P(H)$ and $b_P(H)$ are, with a good precision, linear functions of H (the subscript "P" indicates the relation to the persistent case):

$$a_P(H) = a'_P + a''_P H,$$
$$b_P(H) = b'_P + b''_P H,$$

where $a'_P = -1.680$, $a''_P = 4.869$, $b'_P = 1.051$ and $b''_P = -0.399$.

The mean escape time dependence on the Hurst parameter is shown in Fig. 8.

As expected, the escape times probability density function in the persistent case is also exponential of the form of Eq (13) (see Fig. 9).

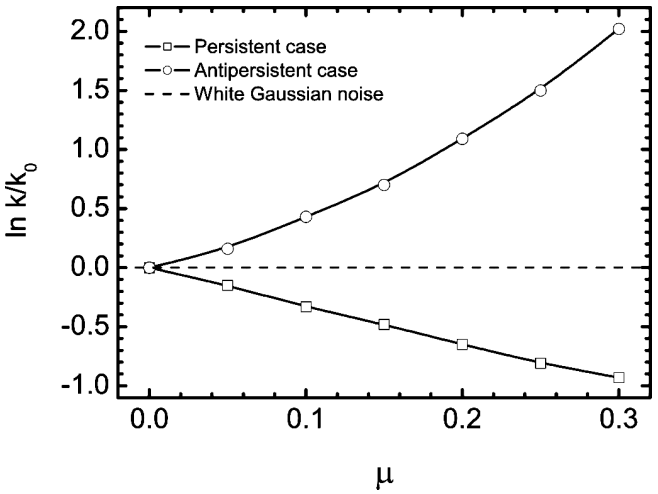

Fig. 10. Relative escape rate $k(H)/k(H=1/2)$ as a function of $\mu = |H - 1/2|$ in the persistent case (squares) and the antipersistent case (circles). The solid parabolic and straight lines stand for fitting the results with Eqs. (10) and (14), respectively

5. Conclusions

We have considered the Kramers problem for the fractional Brownian motion. Using the method of numerical integration of the overdamped Langevin equation with a fractional Gaussian random source, we have shown that, similarly to the classical result presented, e.g., in [7], the dependence of the mean escape time from a truncated harmonic potential on the noise intensity is exponential, both for the persistent and antipersistent cases. This contradicts the conclusion made in [32], where the stretched exponential behavior of the escape time probability density function was reported. The escape time probability density function also behaves qualitatively in the same manner as that of the classical Brownian particle.

An important phenomenon is revealed when considering the diffusion rate. Let us introduce the escape rate $k = 1/T_{\rm esc}$ and make a comparison of the escape rate with the classical Kramers one. Figure 10 indicates that, in the persistent case, the escape rate is smaller than the classical one, and we have a subdiffusion phenomenon. On the contrary, when dealing with the free fractional Brownian motion, the mean squared displacement is $\left\langle x^2(t)\right\rangle = 2D|t|^{2H}$ (the larger the value of H, the faster the particle) and thus, the persistent noise gives birth to the superdiffusivity. The same picture arises in the antipersistent case, but *vice versa*: for the free fractional Brownian motion, we have the subdiffusion, while the walks inside a harmonic potential are superdiffusive. However, such an event is in accordance with Molchan's analytics [35] discussed in Section 2.

At the end, we would like to mention some very promising applications of the numerical results obtained here. Namely, the model studied in this paper is relevant for a number of real physical systems described with continuum elastic models such as flexible and semiflexible polymers [36–38], membranes [37, 39–41], growing interfaces [42–46], fluctuating surfaces [47], and diffusion-noise systems [48]. Indeed, it was shown very recently that the Generalized Elastic Model suited for the description of the systems listed above yields the Langevin description with a fractional Gaussian noise [49–51].

The authors acknowledge the discussions with J. Klafter, R. Metzler, and I. Sokolov. AVC acknowledges the financial support from the MC IIF Programme, grant "LeFrac".

1. *Noise in Nonlinear Dynamical Systems*, edited by F. Moss and McClintock (Cambridge University Press, Cambridge, 1989).
2. P. Hänggi, P. Talkner, and M. Bokrovec, Rev. Mod. Phys. **62**, 251 (1990).
3. S. Arrhenius, Z. Phys. Chem. **4**, 226 (1889).
4. M.V. Smoluchowski, Ann. Phys. **21**, 756 (1906).
5. L.A. Pontryagin, A.A. Andronov, and A.A. Vitt, Zh. Eksp. Teor. Fiz. **3**, 165 (1933).
6. H.A. Kramers, Physica A **7**, 284 (1940).
7. S. Chandrasekhar, Rev. Mod. Phys. **15**, 1 (1943).
8. A.N. Malakhov, Chaos **7**, 3 (1997).
9. Y. Sinai, Theor. Prob. Appl. **27**, 256 (1982).
10. L.F. Richardson, Proc. Roy. Soc. London A **110**, 709 (1926).
11. G. Boffetta and I.M. Sokolov, Phys. Rev. Lett. **88**, 094501 (2002).
12. H. Scher and E.W. Montroll, Phys. Rev. B **12**, 2455 (1975).
13. G. Pfister and H. Scher, Adv. Phys. **27**, 747 (1978); Q. Gu, E.A. Schiff, S. Grebner, and R. Schwartz, Phys. Rev. Lett. **76**, 3196 (1996).
14. A. Caspi, R. Granek, and M. Elbaum, Phys. Rev. Lett. **85**, 5655 (2000).
15. A. Caspi, R. Granek, and M. Elbaum, Phys. Rev. E **66**, 011916 (2002).
16. H. Scher, G. Margolin, R. Metzler, J. Klafter, and B. Berkowitz, Geophys. Res. Lett. **29**, 1061 (2002); B. Berkowitz, A. Cortis, M. Dentz, and H. Scher, Rev. Geophys. **44**, RG2003 (2006).
17. P.D. Ditlevsen, Phys. Rev. E **60**, 172 (1999).

18. A.V. Chechkin, J. Klafter, and I.M Sokolov, Europhys. Lett. **63**, 3 (2003).
19. P. Imkeller and I.J. Pavlyukevich, Phys. A **39**, L237 (2006); P. Imkeller and I. Pavlyukevich, Stoch. Proc. Appl. **116**, 611 (2006).
20. A.V. Chechkin, O.Yu. Sliusarenko, R. Metzler, and J. Klafter, Phys. Rev. E **75**, 041101 (2007).
21. A.N. Kolmogorov, Dokl. Acad. Sci. USSR **26** 115 (1940).
22. B.B. Mandelbrot and J.W. van Ness, SIAM Rev. **1** 422 (1968).
23. D. Panja, E-print arXiv:0912.2331.
24. L. Lizana and T. Ambjörnsson, Phys. Rev. Lett. **100**, 200601 (2008); Phys. Rev. E **80**, 051103 (2009).
25. G. Guigas and M. Weiss, Biophys. J. **94**, 90 (2008); J. Szymanski and M. Weiss, Phys. Rev. Lett. **103**, 038102 (2009); V. Tejedor *et al.*, Biophys J. (at press).
26. H.E. Hurst, Trans. Amer. Soc. Civil Eng. **116**, 400 (1951).
27. T.N. Palmer, G.J. Shutts, R. Hagedorn, F.J. Doblas-Reyes, T. Jung, and M. Leutbecher, Ann. Rev. Earth Planet. Sci. **33**, 163 (2005).
28. I. Simonsen, Physica A **322**, 597 (2003); N.E. Frangos, S.D. Vrontos, and A.N. Yannacopoulos, Appl. Stochast. Models in Business and Industry **23**, 403 (2007).
29. T. Mikosch, S. Rednick, H. Rootzén, and A. Stegemann, Ann. Appl. Prob. **12**, 23 (2002).
30. I. Goychuk and P. Hänggi, Phys. Rev. Lett. **99**, 200601 (2007).
31. I. Goychuk, arXiv:0905.0826v3 (2009).
32. A.H. Romero, J.M. Sancho, and K. Lindenberg, Fluct. and Noise Lett. **2**, 2 (2002).
33. B.S. Lowen, Meth. Comput. Applied Probab. **1:4**, 445 (1999).
34. G. Samorodnitsky and M.S. Taqqu, *Stable Non-Gaussian Random Processes* (Chapman & Hall, New York, 1994).
35. G.M. Molchan, Commun. Math. Phys. **205** 97 (1999).
36. M. Doi and S.F. Edwards, *The Theory of Polymer Dynamics* (Clarendon Press, Oxford, 1986).
37. R. Granek, J. Phys. II France **7**, 1761 (1997).
38. E. Farge and A.C. Maggs, Macromol. **26**, 5041 (1993); A. Caspi *et al.*, Phys. Rev. Lett. **80**, 1106 (1998); F. Amblard *et al.*, Phys. Rev. Lett. **77**, 4470 (1996).
39. E. Freyssingeas, D. Roux, and F. Nallet, J. Phys. II France **7**, 913 (1997); E. Helfer *et al.*, Phys. Rev. Lett. **85**, 457 (2000).
40. R. Granek and J. Klafter, Europhys. Lett. **56**, 15 (2001).
41. A.G. Zilman and R. Granek, Chem. Phys. **284**, 195 (2002).
42. S.N. Majumdar and A. Bray, Phys. Rev. Lett. **86**, 3700 (2001).
43. J. Krug *et al.*, Phys. Rev. E **56**, 2702 (1997).
44. S.F. Edwards and D.R. Wilkingson, Proc. R. Soc. London A **381**, 17 (1982).
45. H. Gao and J.R. Rice, J. Appl. Mech. **65**, 828 (1989).
46. J.F. Joanny and P.G. de Gennes, J. Chem. Phys. **81**, 552 (1984).
47. Z. Toroczkai and E.D. Williams, Phys. Today **52**, No. 12, 24 (1998).
48. N.G. van Kampen, *Stochastic Processes in Chemistry and Physics* (North-Holland, Amsterdam, 1981).
49. A. Taloni and M.A. Lomholt, Phys. Rev E **78**, 051116 (2008).
50. L. Lizana *et al.*, ArXiv preprint arXiv:0909.0881 (2009).
51. A. Taloni, A.Chechkin, and J. Klafter, Phys. Rev. Lett. (2010) (accepted).

Received 08.10.09

ПРОХОДЖЕННЯ ЧЕРЕЗ БАР'ЄР, ЗУМОВЛЕНЕ ДРОБОВИМ ГАУСОВИМ ШУМОМ

О.Ю. Слюсаренко, В.Ю. Гончар, О.В. Чечкін

Р е з ю м е

За допомогою чисельного інтегрування передемпфованого рівняння Ланжевена досліджено задачу про швидкість вильоту частинки із потенціальної ями під дією дробового гаусового шуму. На прикладі обрізаного гармонічного потенціалу отримано залежності середнього часу вильоту від інтенсивності шуму та показника Херста, а також обчислено функції розподілу часів вильоту. Зроблено висновок, що, як і у випадку класичної задачі з білим гаусовим шумом, ці величини є експоненціальними функціями відповідних параметрів.